

Research Article

Optimising reaction variables for the preparation of superabsorbent iron fertiliser hydrogel using sugarcane bagasse: A sustainable approach to improve crop nutrient release

C. Bharaani Sri 

Department of Soil Science and Agricultural Chemistry, Tamil Nadu Agricultural University, Coimbatore - 641003 (Tamil Nadu), India

R. Shanmugasundaram

Department of Soil Science and Agricultural Chemistry, Tamil Nadu Agricultural University, Coimbatore - 641003 (Tamil Nadu), India

S. Marimuthu

Centre for Agricultural Nano Technology, Tamil Nadu Agricultural University, Coimbatore - 641003 (Tamil Nadu), India

T. Chitdeshwari

Department of Soil Science and Agricultural Chemistry, Tamil Nadu Agricultural University, Coimbatore - 641003 (Tamil Nadu), India

A. Senthil

Department of Crop Physiology, Tamil Nadu Agricultural University, Coimbatore - 641003 (Tamil Nadu), India

T. Kalaiselvi

Department of Agricultural Microbiology, Tamil Nadu Agricultural University, Coimbatore - 641003 (Tamil Nadu), India

*Corresponding author. E-mail: bharaanisri@gmail.com

Article Info

<https://doi.org/10.31018/jans.v15i3.4668>

Received: May 4, 2023

Revised: July 28, 2023

Accepted: August 5, 2023

How to Cite

Sri, B. C. *et al.* (2023). Optimising reaction variables for the preparation of superabsorbent iron fertiliser hydrogel using sugarcane bagasse: A sustainable approach to improve crop nutrient release. *Journal of Applied and Natural Science*, 15(3), 945 - 953. <https://doi.org/10.31018/jans.v15i3.4668>

Abstract

Iron (Fe) is a vital micronutrient essential for crop growth and development. Utilisation of bio-based, environmentally friendly functional polymers is inevitable for society. As an alternative to the conventional Fe fertiliser, the present study aimed to synthesise a higher Fe percentage containing hydrogel with organic substances that can facilitate the slow release of nutrients, reduce fertiliser nutrient fixation, and minimise environmental pollution. The reaction variables were optimised for the preparation of superabsorbent using sugarcane bagasse and nano-zeolite-based slow-release Fe fertiliser (SR Fe) hydrogel. This was formulated by graft, co-polymerising acrylic acid, acrylamide, sugarcane bagasse, and nano-zeolite with N,N'-methylene bis-acrylamide as a crosslinker and ammonium persulfate as an initiator. Based on the swelling percentage, the reaction variables of the SR Fe fertiliser were standardised. The crosslinker (MBA - 10 wt%), the initiator (APS - 10 wt%), the filler (Nano-zeolite - 10 wt%), the monomer acrylamide composition (AAM - 2g), the acrylic acid content (AA - 7 ml), the reaction temperature (60°C), and the drying temperature (40°C) were chosen based on desirable swelling percentage and loaded with Fe fertiliser. The Fe fertiliser was loaded to sugarcane bagasse in different ratios (1:0.5, 1:1, 1:1.5, 1:2). The present study showed that the SR Fe fertiliser with the highest percentage of Fe (6.4%) in the ratio of sugarcane bagasse to Fe fertiliser of 1:2 could be used as an effective SR Fe fertiliser to supply nutrients slowly to crops to meet their nutrient needs and improve nutrient use efficiency.

Keywords: Iron, Sugarcane Bagasse, Superabsorbent hydrogel, Swelling percentage

INTRODUCTION

Slow-release fertiliser (SRF) formulations were created to address environmental issues posed by water-

soluble fertilisers. SRF formulations minimise fertiliser dose, losses, and environmental damage. Superabsorbent hydrogels (SHs) have become popular for encapsulating or holding soluble nutrients in SRF formula-

tions (Anas *et al.*, 2020). SHs are made of a three-dimensional crosslinked polymeric network that absorbs and retains a significant amount of aqueous or biological fluids (Firmanda *et al.*, 2022). For high-quality, high-yield crops, the soil must have enough iron (Fe) micro-nutrients in addition to main nutrients like nitrogen (N), phosphorous (P), and potassium (K). However, the low solubility of Fe in calcareous soils lowers its availability for plants. Thus, these plants have iron-deficient chlorosis due to poor Fe uptake and utilisation (Arif *et al.*, 2022). Due to this nutritional problem, plants release natural organic compounds into the rhizosphere to complex and absorb Fe from the soil. Due to the high Fe deficiency, this technique may not give enough Fe for plants in calcareous soils. Applying soluble ferric ion fertilisers to the soil or directly onto the plant foliage is recommended to prevent or manage iron-deficient chlorosis. Due to their high-water solubility, irrigation and rains can leach these Fe fertilisers from soil strata. Fe fertilisers must be applied often to the soil to provide an effective concentration of Fe ions at the root zone. Routine Fe fertiliser supply increases fertiliser use, which wastes fertiliser, uses more energy, and raises expenses (Kalyan *et al.*, 2021). A novel slow-release Fe fertiliser formulation based on SHs can improve plant iron nutrition, reduce fertiliser loss, and reduce groundwater contamination. Synthetic acrylate monomers make up most SHs, but their high production cost and environmental effect have limited their use. Because of their particular commercial and environmental benefits, multicomponent SHs made of acrylate monomers and polysaccharides that are naturally occurring are of tremendous interest (Thivya *et al.*, 2022). Chitosan, alginate, starch, and gelatin have been employed to synthesise multicomponent SHs. However, sugarcane bagasse (SB), an agro-industrial byproduct of sugarcane, has been inadequately studied as a cheap and abundant starch source for SH synthesis. SB in SH synthesis increases biodegradability and decreases acrylate-based monomer content (Shariatnia, 2020). SHs can supply agrochemicals, but their high production cost limits their application. Filling SH mixtures with low-cost clay minerals can fix this. Many SRF formulations have been produced, but few have been employed to prevent Fe deficiency-related nutritional problems. The leaching of Fe fertilisers is another key issue that has received less attention. These challenges led us to formulate a novel multinutrient fertiliser by integrating a soluble Fe fertiliser into an SB-based superabsorbent nanocomposite. SB to synthesise SH is a great idea that lowers manufacturing costs and opens new avenues for agro-industrial byproducts (Kumar, 2022). Nano-zeolite's strong hydrophilicity increases the superabsorbent nanocomposite's swelling capacity. Nano-zeolite can also control nutrient release in multinutrient fertiliser formulations (Pimsen *et al.*, 2021). Slow-release fertilis-

er hydrogel performance depends on optimising reaction factors. Thus, the present study aimed to explore best reaction variables affecting hydrogel swelling capacity to prepare superabsorbent slow release Fe fertiliser hydrogel.

MATERIALS AND METHODS

Materials

Sugarcane bagasse (SB) was utilised without further purification after being obtained from an agricultural-based enterprise (EID Parry). The chemicals acrylic acid (AA), acrylamide (AAM), N,N'-methylene bisacrylamide (MBA), ammonium persulfate (APS), ferrous sulphate, and ethanol were purchased from the Merck company. Sigma Aldrich supplied the zeolite. Other agents utilised in this study were of an Analytical grade, and Milli-Q[®] distilled water was used for preparing all solutions.

Methods

Preparation of SB/ Nano-zeolite superabsorbent nanocomposite Fe fertiliser

A suitable amount of ground sugarcane bagasse (1g), an abundantly available agro-industrial byproduct (particle size range = 40–80 mesh) was dissolved in 50 mL of Milli-Q[®] water, followed by adding nano-zeolite while stirring continuously. The resultant suspension was then sonicated with a probe sonicator at 50 W for 5 minutes with 10 seconds on and off cycle, maintaining the temperature at about 32°C and 35% amplitude. Then, it was transferred to a 1000 mL flat-bottom three-neck flask fitted with a reflux condenser, magnetic stirrer with hot plate, a thermometer, and a nitrogen line. After heating the solution to the desired temperature (40°C to 90°C the most desirable temperature with maximum swelling was selected for synthesis)) gradually and purging it with nitrogen to eliminate dissolved oxygen and maintain anaerobic condition, a predetermined amount of APS was added to form starch macro-radicals. A solution with varying quantities of 70% neutralised AA, MBA, and AAM was added to the reaction mixture 10 minutes later. The quantities of inputs and desired temperature leading to high swelling ratio were selected and used for loading Fe fertiliser. FeSO₄ was added in different ratios with respect to sugarcane bagasse after the addition of APS. Throughout the reaction time (approx. 45 min), the desired temperature (varying from 40°C to 90°C) was maintained for the polymerisation process to be completed. The ensuing hydrogel was subsequently cut into small pieces, treated using ethanol to eliminate unreacted species and then dried in a vacuum oven to a constant weight at the desired temperature. Using an atomic absorption spectrophotometer (AAS), the iron content of a synthetic nanocomposite iron fertiliser was measured, and the

percentage of iron in the resulting product was estimated. The schematic representation for the synthesis of SB/Nano-zeolite superabsorbent nanocomposite Fe fertiliser hydrogel is depicted in Fig. 1.

Standardisation of reaction variables based on the swelling percentage

Effect of reaction variables on the swelling percentage

The quantity of sugarcane bagasse (1 g), nano-zeolite (10 wt%), AA (2 g), APS (10 wt%), and Acrylic acid (7 mL) was unaltered, while the quantity of crosslinker was adjusted from 0.25% wt to 30% wt to investigate the effect of crosslinker on swelling. Similarly, the amount of the initiator was changed from 1 weight per cent to 30 weight percent while keeping all other parameters constant. Similarly, to investigate the effect of the filler, the amount was altered from 1% wt to 30% wt, while no other parameters were changed. All other variables were held constant while varying the amount of acrylamide from 0.5 to 3.5 g to observe its impact on swelling. Again, while holding all other variables constant, the amount of acrylic acid was changed from 1 ml to 10 ml to observe its impact on swelling. The temperature was varied from 40°C to 90°C without changing any other parameters to evaluate the reaction temperature's impact on swelling. Parallel to this, the temperature was changed from 40°C to 70°C without changing any other parameters to study the drying temperature's impact on swelling.

Swelling Percentage Calculation of Hydrogels:

Swelling behaviour of SB/Nano-zeolite derived super absorbent polymer was examined by soaking a predetermined amount (0.1g) of hydrogels in deionised water at the ambient temperature to attain the equilibrium condition. The swelled gels were taken out and their exteriors were lightly padded with blotting paper to eliminate extra water on top of the gels, and the mass of the gel was recorded. When there was no variation

in the mass of swollen hydrogels, hydrogels reached their equilibrium condition. The swelling percentage of hydrogels was calculated with the following formula:

$$\text{Swelling percentage (\%)} = \frac{W_2 - W_1}{W_1} \times 100 \quad \text{Eq. 1}$$

W_1 is the weight of dry hydrogel and W_2 is the weight of swollen hydrogel.

Procedure for the estimation of Fe in SR Fe fertiliser hydrogel

To determine the micronutrient Fe content, 2 g of fertiliser sample was transferred to silica basin. The contents were ignited over rose head flame gently during the initial stage and strongly using muffle furnace in later stages to convert the sample to ash. Ignited ash from silica basin was transferred to a 250 ml conical flask with a jet of water and with 5 ml of concentrated H_2SO_4 . The conical flask was covered with funnel after adding 20 ml of concentrated HCl and subjected to digestion. After digestion, the content in the flask was diluted with water, and the insoluble matter was allowed to settle and filtered through Whatman No. 1 filter paper with hot water. The filtrate washing was collected in a 500 ml volumetric flask and the volume was made upto 500 ml with distilled water. The micronutrient Fe content in the sample solution was estimated using an Atomic Absorption Spectrophotometer (Model: Varian SpectrAA 220) (Lindsay and Norvell, 1978).

Calculation:

$$\text{Fe content (ppm)} = \frac{\text{Concentration (A)} \times (\text{Volume of extract made up (ml)})}{\text{Wt. of sample taken for analysis (g)}} \quad \text{Eq. 2}$$

Estimation of encapsulation efficiency

$$\text{Loading efficiency (\%)} = \frac{\text{Product yield obtained during synthesis (g)}}{\text{Fe added through fertiliser (g)}} \times 100 \quad \text{Eq. 3}$$

Incubation experiment to optimise the effect of different ratios of sugarcane bagasse and Fe fertiliser on nutrient release

An incubation experiment was conducted to optimise the effect of different sugarcane bagasse and Fe fertiliser ratios on nutrient release. Hundred grams of processed soil sample was weighed into polythene containers and mixed with the calculated quantities of SR Fe fertilisers with different ratios per treatment. The batch experiments were conducted in Completely Randomised Block Design (CRD) with three replicates. The soil was incubated for 60 days. The soil was maintained at field capacity throughout the incubation period by regular moisture adjustments. Destructive sampling was carried out at 7, 15, 30, 45 and 60 days after incu-

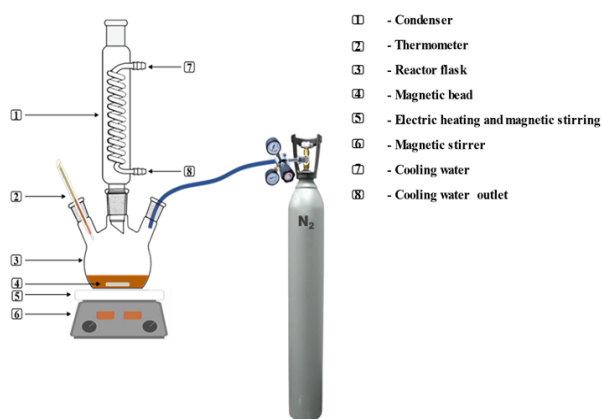


Fig. 1. Schematic representation for the synthesis of slow release nanocomposite iron fertiliser

bation. The treatment schedule included six treatments: T₁ (No Fe), T₂ (Fe as FeSO₄), T₃ (SR Fe fertiliser 1:0.5), T₄ (SR Fe fertiliser 1:1), T₅ (SR Fe fertiliser 1:1.5), and T₆ (SR Fe fertiliser 1:2). The DTPA extractable Fe present in soil samples were estimated using the standard protocol outlined by Lindsay and Norvell (1978).

RESULTS AND DISCUSSION

Effect of crosslinker on the swelling percentage

The amount of crosslinker significantly impacts the hydrogel's distinguishing characteristics. By joining the various polymer chains to create pores inside the polymer matrix, the crosslinker creates a 3D network. The mechanical characteristics of the gel are impacted by the crosslinker concentration, which in turn impacts how well they can swell (Gao *et al.*, 2021). Fig. 2a illustrates how crosslinkers affect the SAH's ability to absorb. The swelling percentage climbed from 265% at 0.25 wt % to 516% at 10 wt % and subsequently declined to 470 %, as indicated when the amount of MBA increased from 0.25 to 30 wt %. With a crosslinker concentration of 10 weight percent, the hydrogel was determined to have the greatest swelling capacity. The swelling ability was reduced after the crosslinker concentration was increased from 10 weight percent to 30 weight percent. This might be because the crosslinking density rises with the crosslinker's concentration, reducing the hydrogel's capacity to swell (Sarmah and Karak, 2020). The distance between the crosslinked points also reduces with an increase in crosslinking density, making the hydrogel harder and more compact. Consequently, the ability of the hydrogel to swell is diminished because the pores between the cross-linked sites cannot be significantly enlarged (El Idrissi *et al.*, 2022). As a result, the area available for water adsorption in pores reduces. The crosslinker can not connect individual polymer sites in lower concentrations to create a stable gel (Qamruzzaman *et al.*, 2022).

Effect of initiator on the swelling percentage

By thermally converting free starch macroradicals, the initiator starts the polymerisation of monomer molecules. The initiator's concentration strongly influences the hydrogel's swelling (Tanan *et al.*, 2019). It was discovered that when the initiator concentration was raised, the swelling capacity was enhanced initially (from 1 to 10 wt%) until it reached 513%, and then it decreased to 397% when the APS concentration was increased to 30 wt%. The maximal SAH swelling occurred at an APS level of 10 wt%, which was regarded as the ideal initiator concentration (Fig. 2b). This was also the lowest concentration of the initiator, below which the hydrogel-forming effects of the polymerisation reaction were ineffective. This might result from a

lack of free radical formation required for the polymerisation process to produce active monomer radicals (Olad *et al.*, 2020). Again, the hydrogel's ability to swell was diminished at initiator concentrations higher than this (10 wt%). This could be due to the production of several free starch macroradicals, which produce numerous active monomer radicals, and the outcomes of numerous tiny polymers (Tanan *et al.*, 2021).

Effect of filler (Nanozeolite) concentration on the swelling percentage

Fig. 2c demonstrates that the absorbency increased to 510 g/g and then dropped as the nano-zeolite content raised from 1 to 30 wt%. This could be because the surface of nanozeolite contains a lot of active OH groups. Nano-zeolite may have exfoliated and scattered during the copolymerisation process, increasing the surface area of the superabsorbent hydrogel and, as a result, the water absorption capacity (Betriani *et al.*, 2023). However, when the amount of nano-zeolite increased, the capacity for storing water in the network was reduced because the more nano-zeolite crosslinking agent reduced the network's available space (Chaisena *et al.*, 2020).

Effect of acrylic acid content on the swelling percentage

Hydrogels with various monomeric concentrations were created to study the impact of monomeric composition on swelling. Fig. 2d depicts the hydrogel's dynamic swelling % at various acrylic acid concentrations. The 7 ml acrylic acid solution had the highest swelling percentage of 512%. Since acrylic acid has a pKa value of 4.28, its chains are collapsed at pH values below 4, which lowers the swelling ratio. Yet, as the pH rises above 6 and 8, acrylic acid produces carboxylate ions that repel one another, causing the swelling ratio to steadily rise. According to findings, gel swelling increased as acrylic acid content increased because more carboxylic groups were available for ionisation (Ghobashy *et al.*, 2022). This led to electrostatic repulsion throughout the chain, which caused the initially coiled molecules to expand. When the pH of the media shifted from lower to higher, hydrogels swelled more (Rop *et al.*, 2019).

Effect of monomer (AAm) content on the swelling percentage

Fig. 2e showed how the amount of Acrylamide (AAm) affected the ability of SAH to absorb water. The maximum absorption capability was noted when the AA content was 2g. The hydrogel's capacity to swell was significantly reduced after the AA content was reduced from 2 to 0.5 g. This might be because there isn't enough AA in the matrix to create the best crosslinked polymer

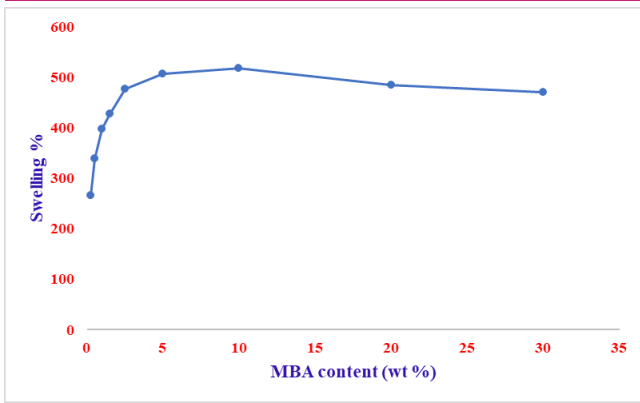


Fig. 2a Effect of crosslinker content on swelling %

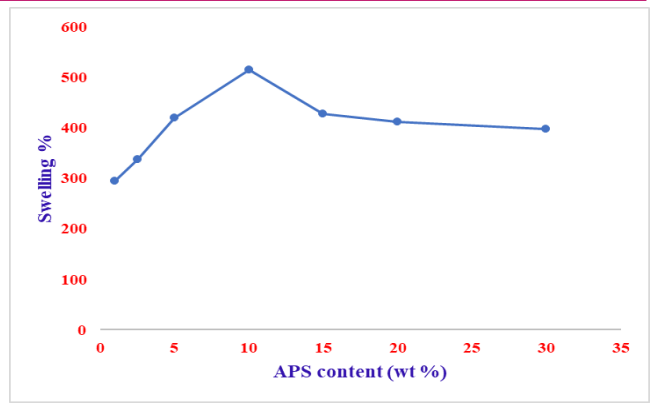


Fig. 2b Effect of initiator content on swelling %

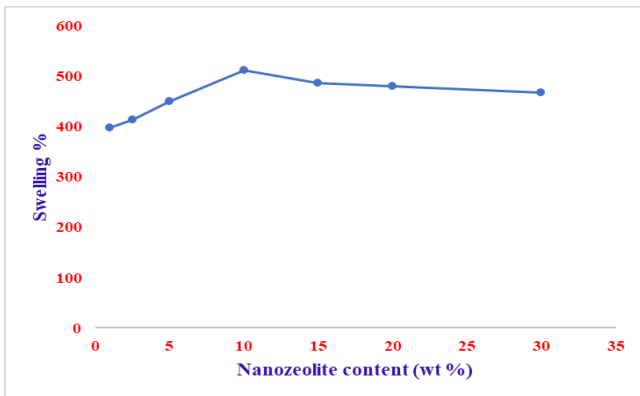


Fig. 2c Effect of filler content on swelling %

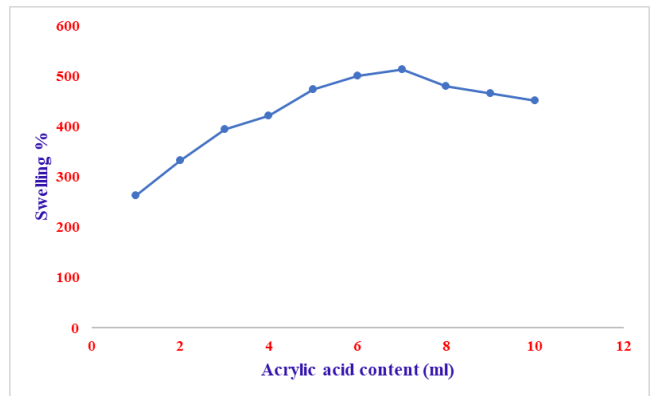


Fig. 2d Effect of acrylic acid content on swelling %

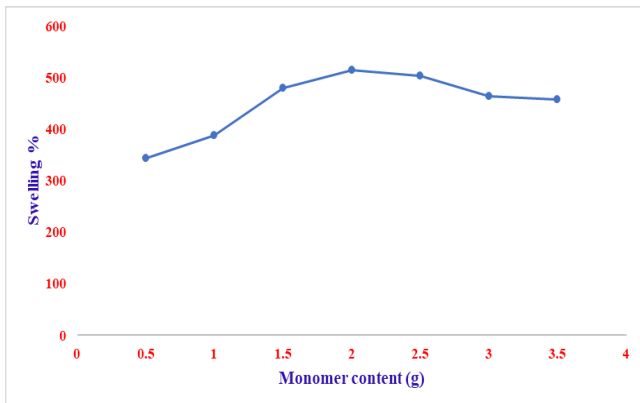


Fig. 2e Effect of monomer (AAm) content on swelling %

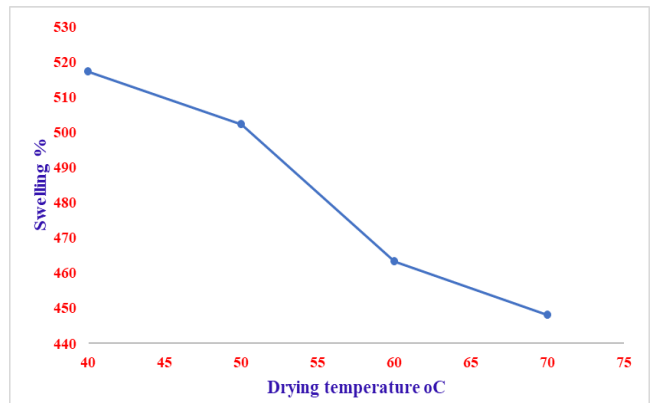


Fig. 2f Effect of drying temperature on swelling %

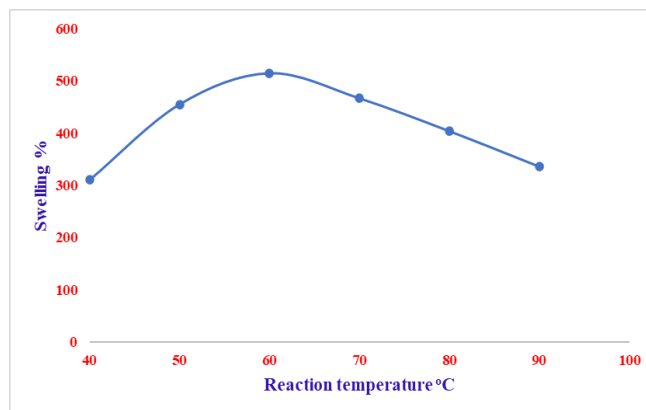


Fig. 2g Effect of reaction temperature on swelling %

chains. This could also be due to the reaction mixture's lower total solid concentration (Daoud and Bennour, 2021). As a result, there is more initiator present, which, as explained earlier, causes the molecular chain length to shorten and lowers the swelling value. Yet, the swelling capacity has risen with adding more AA due to more hydrophilic COO groups on the AA chains (Kumar *et al.*, 2019). However, when the amount of AA was large (2.5 g), the solid concentration in the reaction mixture was equally high. The amount of chain coiling and crosslinking grew along with increased monomer concentration inside the reactor, resulting in a very high degree of polymerisation and an extremely hard hydrogel. As the gel's strength grew, the pores between the crosslinked sites expanded to a limited degree. As a result, there was less space for water molecules (Zhang *et al.*, 2023).

Effect of drying temperature on the swelling percentage

The drying temperature is another crucial element in creating superabsorbent hydrogels (Sharma *et al.*, 2023). Fig. 2f illustrates how the drying temperature affects the swelling behaviour of the superabsorbent nanocomposite fertiliser hydrogels. It demonstrates that the swelling percentage of the hydrogels reduces as the temperature rises, with the largest swelling percentage being observed when the hydrogel was dried to achieve constant weight at a temperature of 40°C. The decrease in swelling with increasing temperature may be attributable to polysaccharide breakdown and thermal crosslinking of polyacrylamide, which can occur at

high temperatures (Chen and Chen, 2019). At high temperatures, the "main chain" of the polysaccharide is anticipated to disintegrate. The disconnection causes the polysaccharide molecular weight (MW) to drop, which in turn causes the hydrogel's swelling to go down. In addition, polyacrylamide thermal crosslinking can lessen the swelling (Azeem *et al.*, 2023).

Effect of reaction temperature on the swelling percentage

The reactions were carried out at various temperatures, spanning from 40 to 90 °C to investigate the impact of temperature on the hydrogel's swelling percentage. The swelling percentage of the hydrogels was enhanced by raising the temperature to 60°C, as shown in Fig. 2g and subsequently, it was decreased. Maximum swelling percentage (515%) was attained at 60 °C. Increasing the number of free radicals produced on the polymer backbone and the likelihood of colliding with macroradicals increases the swelling percentage (Sharma *et al.*, 2021). Yet, the increased radical chain termination at higher temperatures may cause the swelling percentage to fall after 60 °C.

Preparation of SB/Nano-zeolite Superabsorbent nanocomposite iron fertiliser

The most efficient superabsorbent hydrogel was prepared with the appropriate reaction variables and FeSO₄ fertiliser was loaded into the hydrogel. The loading of FeSO₄ fertiliser was done at different ratios of iron fertiliser and sugarcane bagasse. Sugarcane bagasse (SB) and Fe fertiliser ratios of 1:0.5, 1:1, 1:1.5,

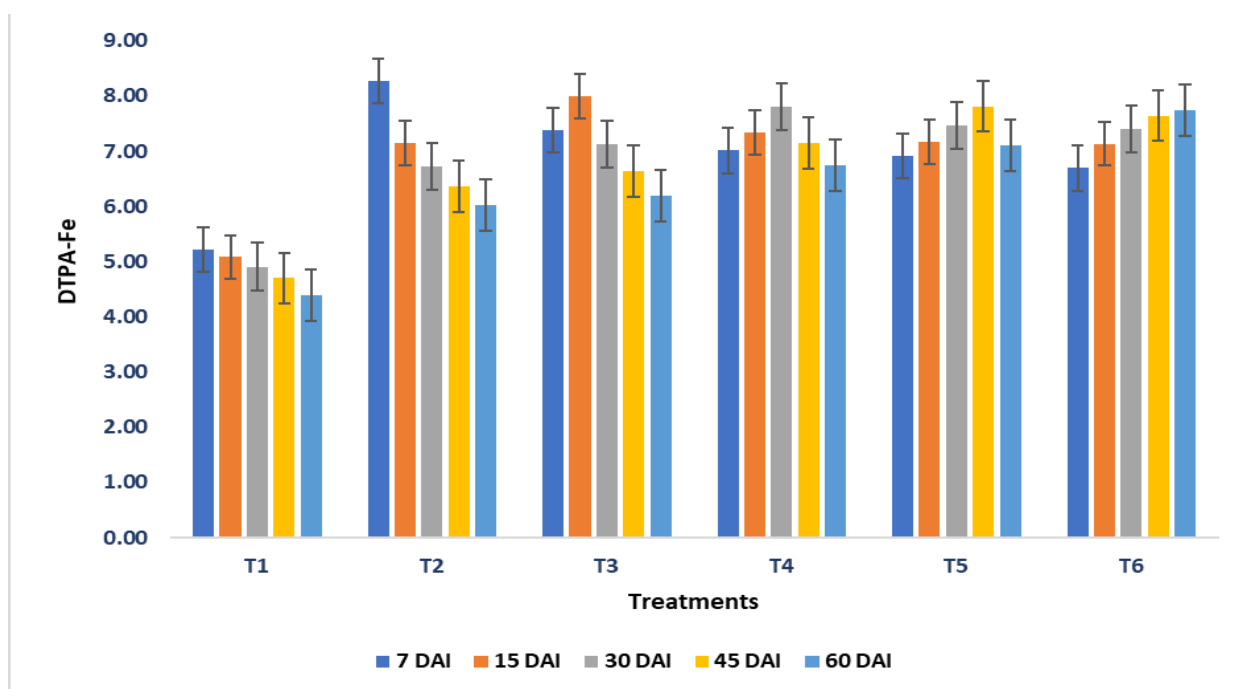


Fig. 3 Effect of slow release nanocomposite iron fertiliser hydrogel on available Fe status of soils at different time intervals

Table 1. Synthesis of nanocomposite iron fertiliser with different ratios and the percentage of Fe, loading efficiency of the synthesised nanocomposite iron fertiliser

Ratio of Sugarcane bagasse and Fe fertiliser (Fertiliser source- FeSO ₄)	% Fe in fertiliser	% Fe in product derived	Loading efficiency (%)
1: 0.5	20	1.6	39
1: 1	20	3.2	40
1: 1.5	20	4.7	39
1: 2	20	6.4	40

and 1:2 resulted in effective hydrogel formation; however, feeding the hydrogel with Fe fertiliser above these ratios was undesirable. Using an atomic absorption spectrophotometer (AAS), the iron content of a synthetic nanocomposite iron fertiliser was measured, and the percentage of iron in the resulting product is shown in Table 1. The percentage of Fe in fertiliser product derived from SB and Fe fertiliser ratio 1:2 was 6.4 %, and the loading efficiency was 40%. As the highest percentage of Fe was found in SB and Fe fertiliser ratio 1:2, this may be used as efficient slow-release iron fertiliser.

Effect of slow-release nanocomposite iron fertiliser hydrogel on available Fe status of soils at different time intervals

Slow-release nanocomposite iron fertiliser had an impact on Fe release in soil (Fig. 3). The initial iron status of the soil used for the incubation experiment was 5.48 mg kg⁻¹. The fertiliser release profile of pure FeSO₄ compound, owing to its ease of dissolution in a soil solution, exhibited a sharp increase in the fertiliser release rate on 7 DAI and then declined. From the results of fertiliser release in soil, it can be inferred that nutrients in the SR Fe fertilisers are liberated slower throughout the incubation period than those in the pure FeSO₄ compound. This might be attributed to the hydrogel's interlinked porous structure facilitating slow nutrient release. These results were in tandem with the results reported by Gharekhani *et al.* (2018), Olad *et al.* (2016) and Rashidzadeh *et al.* (2014).

Conclusion

The SR Fe fertiliser was formulated successfully and involved graft co-polymerisation of acrylic acid, acrylamide, sugarcane bagasse, and nano-zeolite with N,N'-methylene bis-acrylamide as a crosslinker and ammonium persulfate as an initiator. The SR Fe fertiliser's reaction characteristics were optimised based on the swelling percentage. The crosslinker (MBA - 10%), initiator (APS - 10%), filler (Nano-zeolite - 10%), monomer acrylamide composition (AAm - 2g), acrylic acid content (AA - 7 ml), reaction temperature (60°C), and drying temperature (40°C) were all chosen based on the desired swelling percentage and loaded with Fe fertiliser.

Among different loading ratios of the Fe fertiliser tested concerning sugarcane bagasse, SR Fe fertiliser with the highest concentration of Fe (6.4%) in a 1:2 loading ratio can be used as an efficient slow-release Fe fertiliser to meet crops' nutrient needs and increase nutrient use efficiency,

ACKNOWLEDGEMENTS

The authors thank the Department of Soil Science and Agricultural Chemistry and Centre for Agricultural Nano Technology, Tamilnadu Agricultural University, for providing facilities to conduct the research.

Conflict of interest

The authors declare that they have no conflict of interest.

REFERENCES

- Anas, M., Liao, F., Verma, K. K., Sarwar, M. A., Mahmood, A., Chen, Z.-L., Li, Q., Zeng, X. P., Liu, Y. & Li, Y. R. (2020). Fate of nitrogen in agriculture and environment: agronomic, eco-physiological and molecular approaches to improve nitrogen use efficiency. *Biological Research*, 53(1), 1-20. doi: <https://doi.org/10.1186/s40659-020-00312-4>
- Arif, Y., Singh, P., Siddiqui, H., Naaz, R. & Hayat, S. (2022). Transition metal homeostasis and its role in plant growth and development. *Microbial Biofertilizers Micronutrient Availability: The Role of Zinc in Agriculture Human Health*, 159-178. doi: https://doi.org/10.1007/978-3-030-76609-2_8
- Azeem, M. K., Islam, A., Rizwan, M., Rasool, A., Gul, N., Khan, R. U., Khan, S. M. & Rasheed, T. (2023). Sustainable and environment Friendlier carrageenan-based pH-responsive hydrogels: swelling behavior and controlled release of fertilisers. *Colloid Polymer Science*, 1-11. doi: <https://doi.org/10.1016/j.jbiomac.2019.11.091>
- Betriani, R., Sutarno, S., Kartini, I. & Budiarta, J. (2023). Synthesis of Zeolite/NPK Coated with Cu-Alginate-PVA-Glutaraldehyde as a Slow-Release Fertilizer. *Indonesian Journal of Chemistry*, 23(1), 184-199. doi: <https://doi.org/10.22146/ijc.76205>
- Chaisena, A., Narakaew, S. & Promanan, T. (2020). Rice straw-g-poly (acrylic acid)/nano-zeolite NaX superabsorbent nanocomposites with controlled release of fertiliser nutrients.

6. Chen, Y. C. & Chen, Y. H. (2019). Thermo and pH-responsive methylcellulose and hydroxypropyl methylcellulose hydrogels containing K₂SO₄ for water retention and a controlled-release water-soluble fertiliser. *Science of the Total Environment*, 655(958-967). doi: <https://doi.org/10.1016/j.scitotenv.2018.11.264>
7. Daoud, L. & Bennour, S. (2021). Synthesis and Characterisation of Carboxymethyl Cellulose-Graft-Poly(-co-Crotonic Acid) Hydrogel: Matrix for Ammonium Nitrate Release, as Agrochemical. *Russian Journal of Applied Chemistry*, 94(11), 1499-1512. doi: <https://doi.org/10.1134/S1070427221110057>
8. El Idrissi, A., El Gharrak, A., Achagri, G., Essamlali, Y., Amadine, O., Akil, A., Sair, S. & Zahouily, M. (2022). Synthesis of urea-containing sodium alginate-g-poly (acrylic acid-co-acrylamide) superabsorbent-fertiliser hydrogel reinforced with carboxylated cellulose nanocrystals for efficient water and nitrogen utilisation. *Journal of Environmental Chemical Engineering*, 10(5), 108282. doi: <https://doi.org/10.1016/j.jece.2022.108282>
9. Firmanda, A., Fahma, F., Syamsu, K., Suryanegara, L. & Wood, K. (2022). Controlled/slow release fertiliser based on cellulose composite and its impact on sustainable agriculture. *Biofuels, Bioproducts Biorefining*, 16(6), 1909-1930. doi: <https://doi.org/10.1002/bbb.2433>
10. Gao, Y., Peng, K. & Mitragotri, S. (2021). Covalently Crosslinked hydrogels via step-growth reactions: cross-linking chemistries, polymers, and clinical impact. *Advanced Materials*, 33(25), 2006362. doi: <https://doi.org/10.1002/adma.202006362>
11. Gharekhan, H., Olad, A. & Hosseinzadeh, F. (2018). Iron/NPK agrochemical formulation from superabsorbent nanocomposite based on maize bran and montmorillonite with functions of water uptake and slow-release fertiliser. *New Journal of Chemistry*, 42(16), 13899-13914. doi: <https://doi.org/10.1039/C8NJ01947A>
12. Ghobashy, M. M., Amin, M. A., Nady, N., Meganid, A. S., Alkhursani, S. A., Alshangiti, D. M., Madani, M., Al-Gahtany, S. A. & Zaher, A. A. (2022). Improving impact of poly (starch/acrylic acid) superabsorbent hydrogel on growth and biochemical traits of sunflower under drought stress. *Journal of Polymers the Environment*, 1-11. doi: <https://doi.org/10.1007/s10924-021-02322-z>
13. Kalyan, V. R. K., Meena, S., Jawahar, D. & Karthikeyan, S. (2021). In vitro Screening of Iron Efficient Groundnut Cultivars for Calcareous Soil. *International Journal of Environment and Climate Change*, 10(12), 137-148. doi: <http://dx.doi.org/10.9734/ijec/2020/v10i1230291>
14. Kumar, H. (2022). A review on facile synthesis of nanoparticles made from biomass wastes. *Nanotechnology for Environmental Engineering*, 7(3), 783-796. doi: <https://doi.org/10.1007/s41204-022-00259-9>
15. Kumar, V., Mittal, H. & Alhassan, S. M. (2019). Biodegradable hydrogels of tragacanth gum polysaccharide to improve water retention capacity of soil and environment-friendly controlled release of agrochemicals. *International Journal of Biological Macromolecules*, 132(1252-1261). doi: <https://doi.org/10.1016/j.ijbiomac.2019.04.023>
16. Lindsay, W. L. & Norvell, W. (1978). Development of a DTPA soil test for zinc, iron, manganese, and copper. *Soil science society of America journal*, 42(3), 421-428. doi: <https://doi.org/10.2136/sssaj1978.0361599500420030009x>
17. Olad, A., Doustdar, F. & Gharekhan, H. (2020). Fabrication and characterisation of a starch-based superabsorbent hydrogel composite reinforced with cellulose nanocrystals from potato peel waste. *Colloids Surfaces A: Physicochemical Engineering Aspects*, 601(124962). doi: <https://doi.org/10.1016/j.colsurfa.2020.124962>
18. Olad, A., Gharekhan, H., Mirmohseni, A. & Bybordi, A. (2016). Study on the synergistic effect of clinoptilolite on the swelling kinetic and slow release behavior of maize bran-based superabsorbent nanocomposite. *Journal of Polymer Research*, 23(1-14). doi: <https://doi.org/10.1007/s10965-016-1140-0>
19. Pimsen, R., Porrawatkul, P., Nuengmacha, P., Ramasoot, S. & Chanthai, S. (2021). Efficiency enhancement of slow release of fertiliser using nanozeolite-chitosan/sago starch-based biopolymer composite. *Journal of Coatings Technology Research*, 18(10-11), 1-12. doi: <http://dx.doi.org/10.1007/s11998-021-00495-9>
20. Qamruzzaman, M., Ahmed, F. & Mondal, M. I. H. (2022). An overview on starch-based sustainable hydrogels: Potential applications and aspects. *Journal of Polymers the Environment*, 30(1), 19-50. doi: <https://doi.org/10.1007/s10924-021-02180-9>
21. Rashidzadeh, A., Olad, A., Salari, D. & Reyhanitabar, A. (2014). On the preparation and swelling properties of hydrogel nanocomposite based on sodium alginate-g-poly (acrylic acid-co-acrylamide)/clinoptilolite and its application as slow release fertiliser. *Journal of Polymer Research*, 21(1-15). doi: <https://doi.org/10.1007/s10965-013-0344-9>
22. Rop, K., Mbui, D., Njomo, N., Karuku, G. N., Michira, I. & Ajayi, R. F. (2019). Biodegradable water hyacinth cellulose-graft-poly (ammonium acrylate-co-acrylic acid) polymer hydrogel for potential agricultural application. *Heliyon*, 5(3), e01416. doi: <https://doi.org/10.1016/j.heliyon.2019.e01416>
23. Sarmah, D. & Karak, N. (2020). Biodegradable superabsorbent hydrogel for water holding in soil and controlled release fertiliser. *Journal of Applied Polymer Science*, 137(13), 48-65. doi: <https://doi.org/10.1002/app.48495>
24. Shariatnia, Z. (2020). Biopolymeric nanocomposites in drug delivery. *Advanced Biopolymeric Systems for Drug Delivery*, 233-290. doi: https://doi.org/10.1007/978-3-030-46923-8_10
25. Sharma, H., Yadav, A., Rajendran, N., Abinandan, S., Baskar, G. & Krishnamurthi, T. (2023). Techno-economic process parameter studies for hydrogel composite production from corncob biomass and its application as fertiliser releasing agent. *Chemical Papers*, 1-11. doi: <https://doi.org/10.1007/s12010-009-8560-9>
26. Sharma, N., Singh, A. & Dutta, R. K. (2021). Biodegradable fertiliser nanocomposite hydrogel based on poly (vinyl alcohol)/kaolin/diammonium hydrogen phosphate (DAHP) for controlled release of phosphate. *Polymer Bulletin*, 78(2933-2950). doi: <https://doi.org/10.1007/s00289-020-03252-x>
27. Tanan, W., Panichpakdee, J. & Saengsuwan, S. (2019). Novel biodegradable hydrogel based on natural polymers: Synthesis, characterisation, swelling/reswelling and bio-

- degradability. *European Polymer Journal*, 112(678-687). doi: <https://doi.org/10.1016/J.EURPOLYMJ.2018.10.033>
28. Tanan, W., Panichpakdee, J., Suwanakood, P. & Saengsuwan, S. (2021). Biodegradable hydrogels of cassava starch-g-polyacrylic acid/natural rubber/polyvinyl alcohol as environmentally friendly and highly efficient coating material for slow-release urea fertilisers. *Journal of Industrial Engineering Chemistry*, 101(237-252). doi: <https://doi.org/10.1016/j.jiec.2021.06.008>
29. Thivya, P., Akalya, S. & Sinija, V. (2022). A comprehensive review on cellulose-based hydrogel and its potential application in the food industry. *Applied Food Research*, 100161. doi: <https://doi.org/10.1016/j.afres.2022.100161>
30. Zhang, H., Shi, L. W. E. & Zhou, J. (2023). Recent developments of polysaccharide-based double-network hydrogels. *Journal of Polymer Science*, 61(1), 7-43. doi: <https://doi.org/10.1002/pol.20220510>